Conversion of Glycerol to Hydrogen via a Steam Reforming Process over Nickel Catalysts

Sushil Adhikari,[†,‡] Sandun D. Fernando,*[,†] S. D. Filip To,[†] R. Mark Bricka,[§] Philip H. Steele,[||] and Agus Haryanto[†]

Department of Agricultural and Biological Engineering, Mississippi State University, Mississippi State, Mississippi 39762, Department of Chemical Engineering, Mississippi State University, Mississippi State, Mississippi 39762, and Department of Forest Products, Mississippi State University, Mississippi State, Mississippi 39762

Received June 12, 2007. Revised Manuscript Received November 29, 2007

A glut of inexpensive glycerol has resulted from expanding biodiesel production around the world. This glycerol could be used as a good renewable source to produce hydrogen fuel. Hydrogen production from glycerol via a steam reforming process over Ni/CeO_2, Ni/MgO, and Ni/TiO_2 catalysts was studied. The catalysts were characterized by using X-ray diffraction, thermogravimetric analysis, BET surface area analysis, metal dispersion, active surface area analysis, and hydrogen temperature programmed reduction. Ni/CeO_2 had the highest surface area (67.0 m^2/g) followed by Ni/TiO_2 (64.9 m^2/g) and Ni/MgO (50.2 m^2/g). Also, Ni/CeO_2 showed the highest metal dispersion (6.14%) compared to Ni/MgO (0.38%) and Ni/TiO_2 (0.29%). Effects of reaction temperatures, feed flow rates (FFRs), and water/glycerol molar ratios (WGMRs) on hydrogen selectivity and glycerol conversion were analyzed. Ni/CeO_2 was found to be the best performing catalyst compared to Ni/MgO and Ni/TiO_2 under the experimental conditions investigated. Ni/CeO_2 gave the maximum hydrogen selectivity of 74.7% at a WGMR of 12:1, temperature of 600 °C, and FFR of 0.5 mL/min compared to Ni/MgO (38.6%) and Ni/TiO_2 (28.3%) under similar conditions.

Introduction

Currently, alternative energy resources are becoming increasingly important because of dwindling petroleum reserves and increasing environmental concerns. In this regard, biomass is an intriguing candidate because it is renewable and carbon neutral.[1] On the other hand, demand for hydrogen (H_2) is growing due to the technological advancements in the fuel cell industry.[2] Hydrogen can be produced from biobased resources via steam reforming,[3] gasification,[4] and aqueous-phase reforming[5,6] processes. With ever-increasing production of biodiesel, a surplus of inexpensive glycerol has resulted in the world market. Several alternatives are being explored to utilize glycerol, a byproduct from biodiesel plants. For example, several commercial plants have been established recently to produce propylene glycol from glycerol.[7] Producing H_2 from glycerol is another approach that is being investigated in this work.

The glycerol steam reforming process takes place according to the following stoichiometric equation:

$$C_3H_8O_3 + 3H_2O \rightarrow 3CO_2 + 7H_2 \quad (\Delta H^\circ = +346.4\text{kJ/mol}) \tag{1}$$

Several studies[5,8–14] focused on hydrogen production from glycerol. Zhang et al.[14] performed a glycerol steam reforming process over ceria-supported metal catalysts. Results showed that the Ir/CeO_2 catalyst resulted in a complete glycerol

* Corresponding author. Tel.: +1 662 325 3282. Fax: +1 662 325 3853. E-mail address: sf99@abe.msstate.edu.

† Department of Agricultural and Biological Engineering.

‡ Current address: Department of Agricultural and Biosystems Engineering, North Dakota State University, Fargo, North Dakota 58105.

§ Department of Chemical Engineering.

|| Department of Forest Products.

(1) Klass, D. L. *Biomass for renewable energy, fuels, and chemicals*; Academic Press: San Diego, 1998; pp 29–50.

(2) Dunn, S. Hydrogen futures: toward a sustainable energy system. *Int. J. Hydrogen Energy* **2002**, *27*, 235–264.

(3) Deluga, G. A.; Salge, J. R.; Schmidt, L. D.; Verykios, X. E. Renewable hydrogen from ethanol by autothermal reforming. *Science* **2004**, *303* (5660), 993–997.

(4) Hashaikeh, R.; Butler, I. S.; Kozinski, J. A. Selective promotion of catalytic reactions during biomass gasification to hydrogen. *Energy Fuels* **2006**, *20*, 2743–2746.

(5) Cortright, R. D.; Davda, R. R.; Dumesic, J. A. Hydrogen from catalytic reforming of biomass-derived hydrocarbons in liquid water. *Nature* **2002**, *418*, 964–966.

(6) Davda, R. R.; Shabker, J. W.; Huber, G. W.; Cortright, R. D.; Dumesic, J. A. A review of catalytic issues and process conditions for renewable hydrogen and alkanes by aqueous phase reforming of oxygenated hydrocarbons over supported metal catalysts. *Appl. Catal. B: Environ.* **2005**, *56*, 171–186.

(7) Tullo, A. Firms advance chemicals from renewable resources. *Chem. Eng. News* **2006**, 14.

(8) Dauenhauer, P. J.; Salge, J. R.; Schmidt, L. D. Renewable hydrogen by autothermal steam reforming of volatile carbohydrates. *J. Catal.* **2006**, *244*, 238–247.

(9) Soares, R. R.; Simonetti, D. A.; Dumesic, J. A. Glycerol as a source for fuels and chemicals by low-temperature catalytic processing. *Angew. Chem., Int. Ed.* **2006**, *45*, 3982–3985.

(10) Czernik, S.; French, R.; Feik, C.; Chornet, E. Hydrogen by catalytic steam reforming of liquid byproducts from biomass thermoconversion process. *Ind. Eng. Chem. Res.* **2002**, *41*, 4209–4215.

(11) Hirai, T.; Ikenaga, N. O.; Mayake, T.; Suzuki, T. Production of hydrogen by steam reforming of glycerin on Ruthenium catalyst. *Energy Fuels* **2005**, *19*, 1761–1762.

(12) Swami, S. M.; Abraham, M. A. Integrated catalytic process for conversion of biomass to hydrogen. *Energy Fuels* **2006**, *20*, 2616–2622.

(13) Adhikari, S.; Fernando, S.; Haryanto, A. Glycerin steam reforming for hydrogen production. *Trans. ASABE* **2007**, *50* (2), 591–595.

(14) Zhang, B.; Tang, X.; Li, Y.; Xu, Y.; Shen, W. Hydrogen production from steam reforming of ethanol and glycerol over ceria-supported metal catalysts. *Int. J. Hydrogen Energy* **2007**, *32* (13), 2367–2373.

10.1021/ef700520f CCC: $40.75
Published on Web 01/16/2008

conversion at 400 °C; whereas, the complete conversion over Co/CeO_2 and Ni/CeO_2 occurred at 425 and 450 °C, respectively. Similarly, Dauenhauer et al.[8] produced H_2 via an autothermal steam reforming of glycerol over $Rh-Ce/Al_2O_3$ catalyst. Although the autothermal steam reforming process has some advantages over conventional steam reforming,[8] the amount of H_2 produced is less (based on a thermodynamic analysis). Consequently, our study was focused on the steam reforming process.

Hirai et al.[11] reported that steam reforming of glycerol on Ru/Y_2O_3 catalyst exhibited H_2 selectivity of ~90% and complete conversion at 600 °C. Swami and Abraham[12] compared autothermal and conventional steam reforming of the glycerol over γ-Al_2O_3 supported Pd/Ni/Cu/K catalyst. According to them, the autothermal steam reforming process produced a higher amount of H_2, which was in contrast to the previous study.[15] Czernik et al.[10] used a commercial Ni-based reforming catalyst for H_2 production from glycerol; however, detailed results were not reported. Most of the previously mentioned studies focused on expensive noble metal catalysts. Our objective is to explore the possibility of using cheap catalysts for the glycerol steam reforming process.

From our earlier study, we identified Ni as a highly active catalyst for glycerol steam reforming.[16] In this paper, we report the effects of different supports, namely CeO_2, MgO, and TiO_2 on H_2 production and glycerol conversion.

Experimental Details

Catalyst Preparation. Ni catalysts were prepared over three different supports: (i) CeO_2, (ii) MgO, and (iii) TiO_2 (Nanoscale Materials, Manhattan, KS). Catalysts were prepared by the incipient wetness technique using nickel nitrate hexahydrate $[Ni(NO_3)_2 \cdot 6H_2O]$ purchased from Sigma-Aldrich (St. Louis, MO). Metal precursor was impregnated directly into the sieved (16–35 U.S. sieve size) supports. Catalysts were dried at 110 °C for 12 h and calcined at 500 °C for 6 h in air. Furnace temperatures were ramped at 10 °C/min for catalyst calcination and drying. After drying, catalyst samples were sieved again and the 16–35 mesh fraction was used for analysis. Nickel loading was measured using an inductively coupled plasma-optical emission spectrometer (ICP-OES) after the catalyst calcination.

Catalyst Characterization. Catalysts were characterized by the following techniques. Thermogravimetric analysis (TGA) experiments were performed on a TG/DTA 6300 (Perkin-Elmer Instrument, Wellesley, MA). This system is capable of measuring the change in mass of a sample and heat flow as a function of temperature up to 1200 °C. The calcination temperature used for different catalysts was based on the results from TGA. For each catalyst sample, nitrogen (N_2) gas was passed through the instrument at 20 mL/min, and the temperature was ramped at 10 °C/min from room temperature to 1000 °C. Carbon formation on the catalysts was measured by using TGA (TGA-50H, Shimadzu Scientific Instruments, Columbia, MD) by flowing air at 50 mL/min. Catalysts weight loss during TGA was attributed to the carbon formation on the catalysts. X-ray diffraction (XRD) analysis was done at AMIA Laboratories (Leesburg, VA). XRD patterns were recorded using a Rigaku Ultima III diffractor with Cu Kα radiation operated at 40 kV and 44 mA. The starting and end angles were 0.5 and 80°, respectively, with an increment of 0.03°. Catalyst surface area, active metal surface area, and metal dispersion were measured using

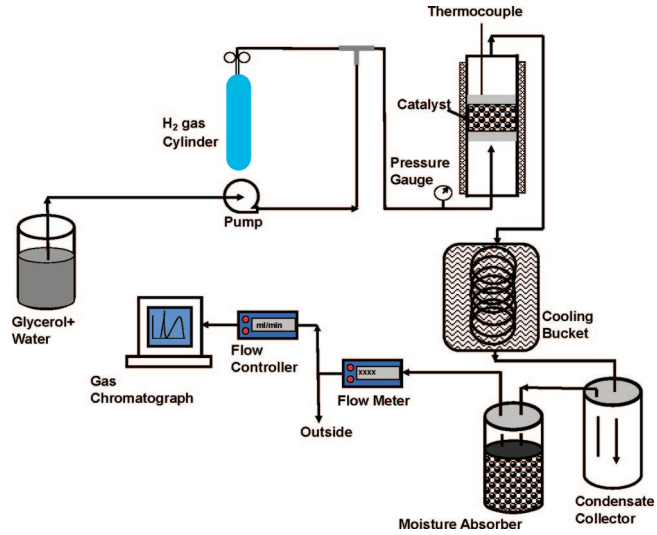

Figure 1. Schematic of the glycerol steam reforming system.

Autosorb-1C (Quantachrome, Boynton Beach, FL). Catalysts surface area was measured by the Brunauer, Emmett, and Teller (BET) method using N_2 adsorption isotherms. Prior to surface area measurement, samples were degassed at 300 °C for 3 h. For chemisorption analysis, samples were heated at 150 °C for 30 min by flowing helium. After drying, catalysts were reduced by flowing H_2 for 2 h at 400 °C and the temperature was ramped at 20 °C/min. Following the reduction of catalyst samples with H_2, subsequent evacuation for two hours was done. The active metal surface area and Ni dispersion were measured using H_2 chemisorption at 40 °C. The percentage of Ni dispersion was calculated by using an H/Ni atomic ratio of one.[17] The average particle diameter was calculated based on the following relation:[17]

$$\text{Average particle diameter} = \frac{\text{Percentage of the metal loading} \times \text{Shape factor } (=6)}{100 \times \text{Surface area of the metal} \times \text{Density of the metal}} \quad (2)$$

Hydrogen temperature programmed reduction (TPR) measurements were performed with an Autosorb-1C equipped with a thermal conductivity detector (TCD). For each measurement, about 250 mg of catalysts (16–35 mesh) were heated to 150 °C under N_2 gas flow (50 mL/min) for 1 h, and then, the samples were cooled to 40 °C. The furnace temperature was programmed to reach 900 at 20 °C/min while flowing 5 vol% of H_2 in N_2 at 35 mL/min. Nickel loading on the catalysts were measured using ICP-OES (Optima 4300 DV, Perkin-Elmer, Waltham, MA). Samples were mixed with sodium peroxide and sodium hydroxide, heated at 600 °C, and rinsed with deionized water and hydrochloric acid in preparation for ICP-OES analysis.

Catalyst Performance Testing. All experiments were carried out in a tubular furnace that could reach temperatures up to 1100 °C. The tubular reactor was made of stainless steel with a $^1/_2$ in. outer diameter and 0.083 in. wall thickness (Swagelok, Pelham, AL). Glycerol and water were mixed in a separate container at preselected molar ratios. The mixture was introduced into the reactor using a high pressure liquid chromatography (HPLC) pump (LC-20AT, Shimadzu Scientific Instrument, Columbia, MD). Catalysts were diluted with an equal amount of fused SiO_2 of similar size and placed in the middle of the tubular reactor by using quartz wool. Prior to the experiment, catalysts were reduced by sending H_2 gas (50 mL/min) for 1 h at 700 °C.

The output gas stream from the reactor was cooled using crushed ice and water. Unreacted water, glycerol, and other liquids formed during the reaction were collected at room temperature, and the condensate was used to analyze glycerol conversion. Figure 1

(15) Rioche, C.; Kulkarni, S.; Meunier, F. C.; Breen, J. P.; Burch, R. Steam reforming of model compounds and fast pyrolysis bio-oil on supported noble metal catalysts. *Appl. Catal. B: Environ.* **2005**, *61* (1–2), 130–139.

(16) Adhikari, S.; Fernando, S.; Haryanto, A. Production of hydrogen by steam reforming of glycerin over alumina supported metal catalysts. *Catal. Today* **2007**, *129* (3–4), 355–364.

(17) Lowell, S.; Shields, J. E.; Thomas, M. A.; Thommes, M. *Characterization of porous solids and powders: surface area, pore size and density*; Kluwer Academic Publishers: Dordecht, 2004; pp 211–233.

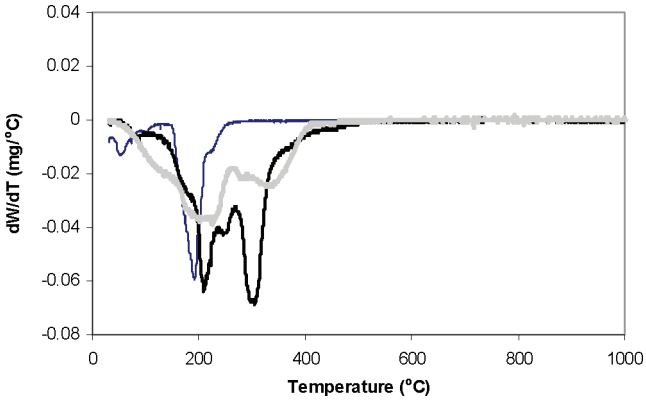

Figure 2. Weight loss profiles of Ni supported on CeO_2 (thick black line), MgO (thin line), and TiO_2 (grey line) during calcination under N_2 gas.

illustrates the glycerol steam reforming process schematic. Hydrogen gas (Figure 1) was used only during the catalyst reduction process. HPLC (1200, Agilent Technologies Inc., Palo Alto, CA) was used to analyze glycerol conversion with a zorbax carbohydrate column (4.6 mm × 150 mm, 5 μm) using a mixture of acetonitrile and water as the mobile phase. Outlet gases were passed through a moisture trap before sending into the gas chromatograph (GC6890 - Agilent Technologies Inc., Palo Alto, CA). The hydrogen content in the gas mixture was analyzed by TCD with an HP-molecular sieve column. Concentrations of carbon monoxide (CO), methane (CH_4), carbon dioxide (CO_2), ethane (C_2H_6), and ethylene (C_2H_4) were analyzed by a flame ionization detector (FID) with an HP-Plot Q column. Altogether, six gases including H_2 were analyzed in this study.

Data Analysis. Catalyst performance is presented in terms of H_2, CO_2, CO, and CH_4 selectivity and glycerol conversion. Performance parameters were calculated based on the following equations:

$$H_2 \text{ selectivity, } \% = \frac{H_2 \text{ moles produced}}{\text{C atoms in the product}} \times \frac{1}{RR} \times 100 \quad (3)$$

where RR is the H_2/CO_2 reforming ratio. In this case of the glycerol steam reforming process, it is $^7/_3$ (eq 1).

$$\text{Selectivity of } i, \% = \frac{\text{C atoms in species } i}{\text{C atoms in the product}} \times 100 \quad (4)$$

where species i = CO, CO_2, and CH_4.

$$\text{Glycerol conversion, } \% = \frac{\text{Glycerol in} - \text{Glycerol out}}{\text{Glycerol in}} \times 100 \quad (5)$$

A completely randomized design[18] was constructed to collect the experimental data. The process was allowed to reach steady state conditions (Figure 5), and all the data were collected after 2 h of operation. Three replications (two samples per replication) were done for each measurement for the analysis. All data reported in this study were averaged from the three replications. Least significance difference (LSD) method with a significance level of $\alpha = 0.05$ was used to determine significant differences in catalysts performance. SAS 9.1 was used for the statistical analysis.[19] Hereafter, the word "significant" refers to a statistical significance at a significance level of $\alpha = 0.05$.

Results and Discussion

The TGA profiles for the Ni catalysts supported on CeO_2, MgO, and TiO_2 are presented in Figure 2. Each catalyst had two peaks corresponding to the weight loss associated with decomposition of nitrates. Peaks were observed in all catalysts before 400 °C, and no weight loss was observed after 500 °C. Consequently, we used calcination temperature of 500 °C in this study. Pure nickel nitrate decomposed to nickel oxide below 400 °C.[20] It was interesting to note that the nickel nitrate decomposed below 300 °C over MgO.

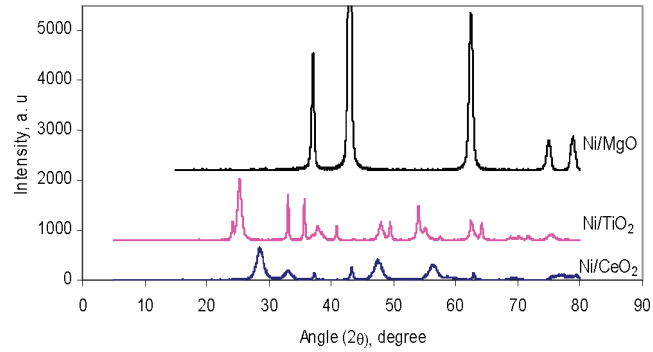

Figure 3. XRD profiles of the selected catalysts calcined at 500 °C.

Table 1. Physisorption and Chemisorption Analysis for the Selected Catalysts

catalyst[a]	BET surface area, m^2/g	active metal surface area, m^2/g	metal dispersion, %	average particle diameter, nm
Ni/CeO_2 (11.6)	67.0	4.74	6.14	16.48
Ni/MgO (9.62)	50.2	0.24	0.38	266.90
Ni/TiO_2 (12.7)	64.9	0.24	0.29	348.50

[a] Values given in the parenthesis are the actual loading of Ni in weight percent.

XRD profiles of Ni/MgO, Ni/TiO_2, and Ni/CeO_2 catalysts calcined at 500 °C are presented in Figure 3. XRD patterns were identified using the software JADE 8 (Materials Data Inc., Livermore, CA). Intensity peaks at 37°, 43°, and 62.4° correspond to MgO while those at 74.9° and 78.8° correspond to $MgNiO_2$. It was difficult to distinguish NiO peaks from MgO because the XRD patterns of NiO and MgO are very close to each other and the NiO concentration was much lower than MgO. With Ni/TiO_2 catalyst, peaks at 24.1°, 33°, 35.6°, 40.8°, 49.4°, 53.9°, 58°, 62.5°, and 64.1° correspond to $Ni(TiO_3)$. Peaks at 25.3°, 38°, 48°, 55°, and 78.8° were identified as TiO_2. Likewise, three peaks at 37.3°, 43.3°, and 62.8° correspond to NiO on Ni/CeO_2, and other peaks were identified as CeO_2.

Physisorption and chemisorption results for different catalysts are given in Table 1. Ni/CeO_2 had the highest BET surface area (67.0 m^2/g) followed by Ni/TiO_2 (64.9 m^2/g) and Ni/MgO (50.2 m^2/g). Also, the active metal surface area (4.74 m^2/g) and metal dispersion (6.14%) were found to be the highest on Ni/CeO_2. The higher metal surface area of Ni/CeO_2 could be due to the better interaction of CeO_2 with nickel precursor. The nickel dispersion on the CeO_2 catalyst prepared in our laboratory was higher than the catalysts prepared by Frusteri et al.[21] and Miyazawa et al.[23] However, the Ni dispersion on the MgO support prepared in our laboratory was found to be lower than

(18) Freund, R. J.; Wilson, W. J. *Statistical Methods*; Academic Press: San Diego, 1997; pp 461–475.
(19) *SAS Software 9.1*; SAS Institute Inc.: Cary, NC, 2003.
(20) Chen, I.; Shiue, D. W. Reduction of nickel-alumina catalysts. *Ind. Eng. Chem. Res.* **1988**, *27*, 429–434.
(21) Frusteri, F.; Freni, S.; Chiodo, V.; Donato, S.; Bonura, G.; Cavallaro, S. Steam and auto-thermal reforming of bio-ethanol over MgO and CeO_2 Ni supported catalysts. *Int. J. Hydrogen Energy* **2006**, *31* (5), 2193–2199.
(22) Furusawa, T.; Sato, T.; Sugito, H.; Miura, Y.; Ishiyama, Y.; Sato, M.; Itoh, N.; Suzuki, N. Hydrogen production from the gasification of lignin with nickel catalysts in supercritical water. *Int. J. Hydrogen Energy* **2007**, *32* (6), 699–704.
(23) Miyazawa, T.; Kimura, T.; Nishikawa, J.; Kado, S.; Kunimori, K.; Tomishige, K. Catalytic performance of supported Ni catalysts in partial oxidation and steam reforming of tar derived from the pyrolysis of wood biomass. *Catal. Today* **2006**, *115*, 254–262.

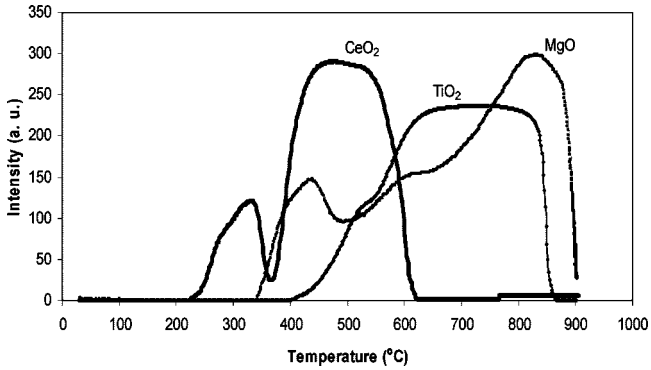

Figure 4. H_2 TPR measurements of the selected catalysts.

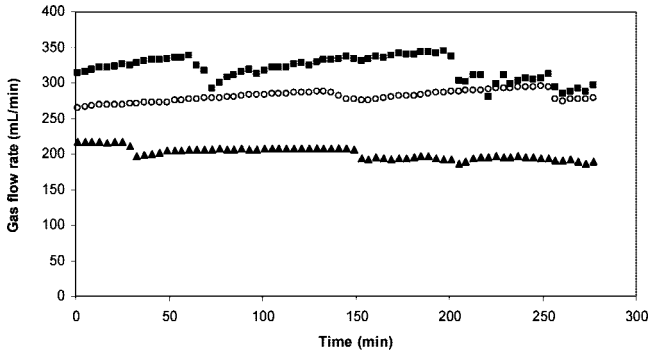

Figure 5. Gas flow rate over CeO_2 (■), MgO (○), and TiO_2 (▲) supported nickel catalyst at an FFR (feed flow rate) of 0.5 mL/min, catalyst loading of 1.5 g, and WGMR (water/glycerol flow rate) of 6:1.

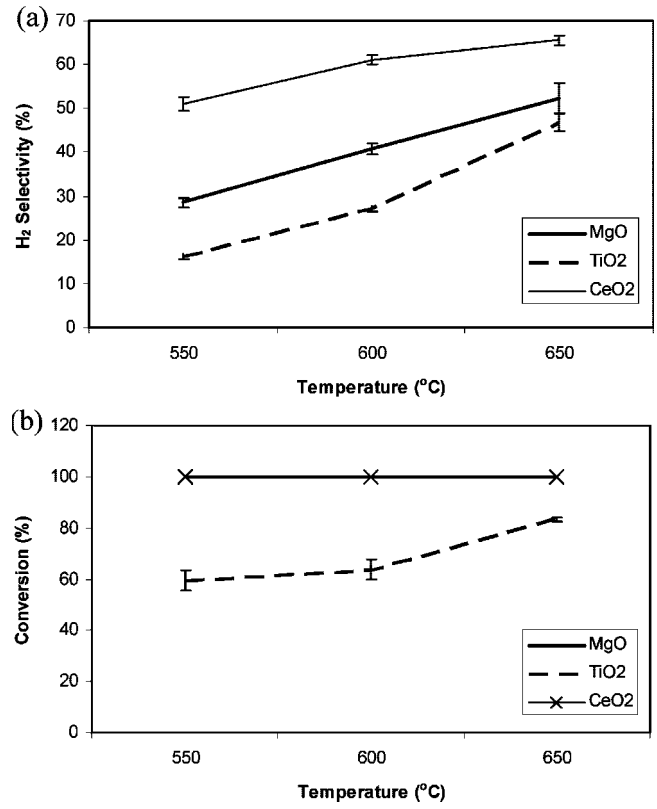

Figure 6. Effect of temperature on (a) H_2 selectivity and (b) glycerol conversion at an FFR of 0.5 mL/min, catalyst loading of 1.5 g, and WGMR of 6:1 [error bars equal 95% confidence interval (CI)].

the catalyst prepared by Frusteri et al.[21] and comparable with the catalyst reported in other studies.[22,23] Likewise, the Ni dispersion on TiO_2 was also lower in our catalyst than was reported by Miyazawa et al.[23] Ni/TiO_2 had the highest metal loading of 12.7 wt % followed by Ni/CeO_2 (11.6 wt %) and Ni/MgO (9.62 wt %).

TPR measurements using H_2 are illustrated in Figure 4. Two reduction peaks around 450 and 825 °C were found for Ni/MgO. The first peak could be attributed to the reduction of NiO located on the surface of MgO. Similarly, the second peak represents the reduction of Ni^{2+} ions located in the MgO lattice. As a result of NiO−MgO bulk solid formation, the oxidized Ni form is reducible only when the reduction temperature is > 550 °C.[24] Freni et al.[24] reported three reduction peaks at 280, 540, and 730 °C on Ni/MgO. Frusteri et al.[25] observed two reduction peaks at 248 and 728 °C over Ni/MgO in another study. Furusawa et al.[22] reported their TPR reduction peaks at 427 and 877 °C with Ni/MgO. Some differences in the reduction temperature might have occurred due to the difference in catalyst preparation methods, which resulted in different oxide formations. Beyond the scope of this study, a more in-depth analysis would be required to identify the differences in reduction peaks over the same catalyst. On Ni/CeO_2, two reduction peaks were found at 325 and 500 °C. The first and second peaks can be attributed to the surface NiO and surface ceria reductions, respectively. Hydrogen TPR was also performed with blank ceria to confirm that ceria can be reduced at 500 °C. Zhang et al.[14] reported two reduction peaks at 320 and 540 °C for Ni/CeO_2. The reduction peak for the Ni/TiO_2 was different from the results reported by Wu et al.[26] The reduction peak pattern for Ni/TiO_2 in our study was found to be similar to the study carried out by Miyazawa et al.[23] A wide reduction peak could be attributed to the reduction of surface TiO_2 and $Ni(TiO_3)$.

Figure 5 illustrates the gas flow rate over three catalysts for about 4 h. Ni/CeO_2 and Ni/TiO_2 suffered from slow deactivation while Ni/MgO did not deactivate during the same period. Initially, Ni/CeO_2 gave the highest gas flow rate followed by Ni/MgO and Ni/TiO_2. After 4 h, gas flow rates over Ni/CeO_2 and Ni/MgO were almost equal. As mentioned earlier, data were collected after 2 h of operation for the analysis.

Hydrogen selectivity increased with an increase in temperature (see Figure 6a). The maximum H_2 selectivity was found to be 66% for Ni/CeO_2 followed by 52% for Ni/MgO and 47% for Ni/TiO_2 at 650 °C. An increase in temperature from 550 to 600 °C and 600 to 650 °C increased H_2 selectivity significantly in all the catalysts. Ni/CeO_2 showed the highest H_2 selectivity followed by Ni/MgO and Ni/TiO_2 in all temperatures investigated. We obtained a complete conversion with Ni/CeO_2 and Ni/MgO at all temperatures investigated in this study. Glycerol conversion increased as the reaction temperature increased, reaching 83% at 650 °C over Ni/TiO_2 (Figure 6b). The change in glycerol conversion was not significant with the increase in temperature from 550 to 600 °C. However, it increased significantly with an increase in temperature from 600 to 650 °C. Glycerol

(24) Freni, S.; Cavallaro, S.; Mondello, N.; Spadaro, L.; Frusteri, F. Production of hydrogen for MC fuel cell by steam reforming of ethanol over MgO supported Ni and Co catalysts. *Catal. Commun.* **2003**, *4* (6), 259–268.

(25) Frusteri, F.; Freni, S.; Chiodo, V.; Spadaro, L.; Blasi, O. D.; Bonura, G.; Cavallaro, S. Steam reforming of bio-ethanol on alkali-doped Ni/MgO catalysts: hydrogen production for MC fuel cell. *Appl. Catal. A: Gen.* **2004**, *270* (1−2), 1–7.

(26) Wu, T.; Yan, Q.; Wan, H. Partial oxidation of methane to hydrogen and carbon monoxide over a Ni/TiO_2 catalyst. *J. Mol. Catal. A: Chem.* **2005**, *226*, 41–48.

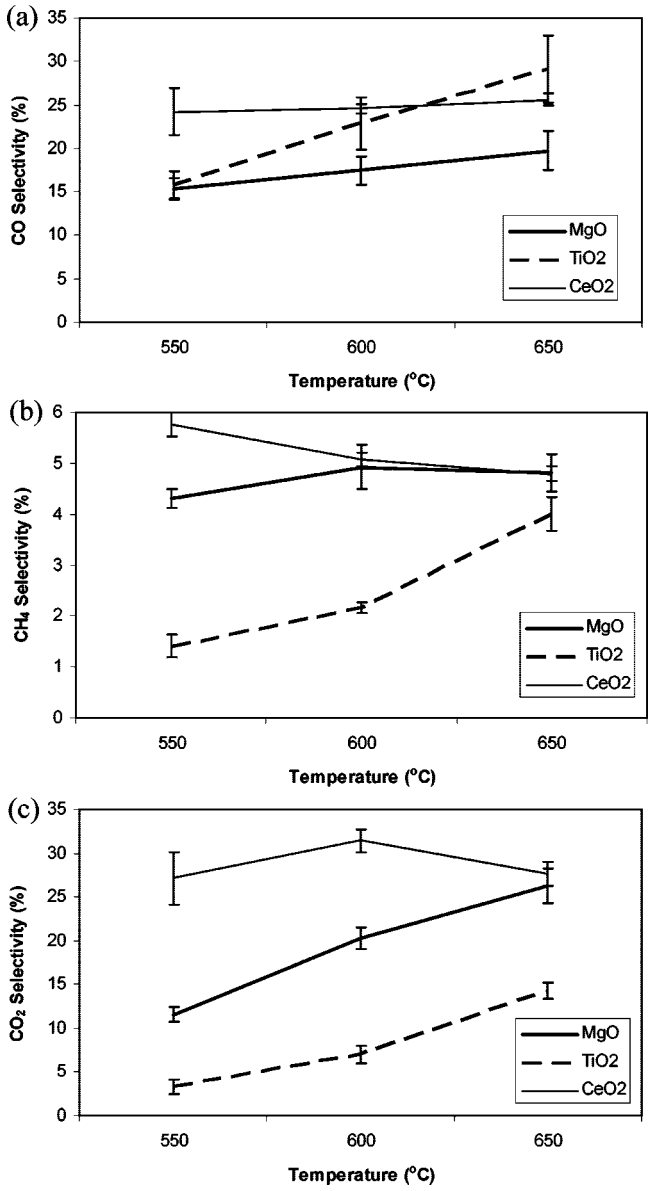

Figure 7. Effect of temperature on (a) CO selectivity, (b) CH_4 selectivity, and (c) CO_2 selectivity at an FFR of 0.5 mL/min, catalyst loading of 1.5 g, and WGMR of 6:1 (error bars equal 95% CI).

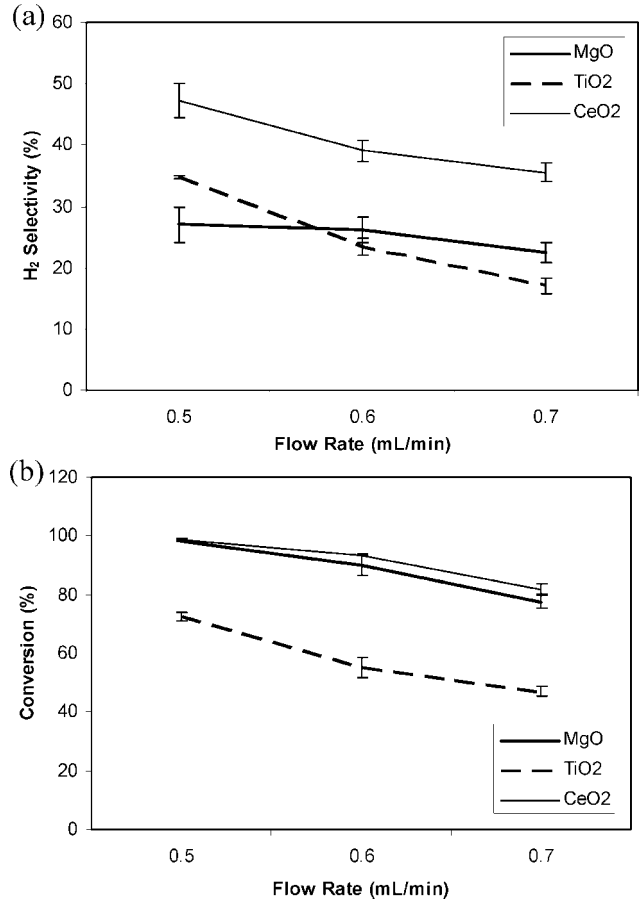

Figure 8. Effect of FFR on (a) H_2 selectivity and (b) glycerol conversion at 600 °C, catalyst loading of 0.75 g and WGMR of 6:1 (error bars equal 95% CI).

conversion was found to be the lowest over Ni/TiO_2 at all temperatures compared to Ni/CeO_2 and Ni/MgO.

Figure 7 depicts CO, CH_4, and CO_2 selectivities at the selected temperatures. CO selectivity did not increase significantly with increase in temperature from 550 to 650 at 50 °C increments on Ni/MgO and Ni/CeO_2. However, there was a significant change in CO selectivity between 550 and 650 °C. Although CO selectivity remained constant on Ni/CeO_2, hydrogen selectivity increased as the reaction temperature increased. The increase in H_2 selectivity could be mainly due to the CH_4 reforming process. CO selectivity increased significantly with increase in temperature over Ni/TiO_2. This is mainly due to the increase in glycerol conversion as the temperature increased. About 25.5% of CO selectivity was observed with Ni/CeO_2 at 650 °C compared to 29.1% with Ni/TiO_2 and 19.7% with Ni/MgO. The concentration of CO in the gas mixture was very high to meet the specification required for the proton exchange member (PEM) fuel cell. Its concentration has to be lower than 10 ppm for the PEM fuel cell. Methane selectivity increased significantly with the increase in temperature from 550 to 600 °C over Ni/MgO. No significant change was found in CH_4 selectivity with further increase in temperature from 600 to 650 °C. Similarly, CH_4 selectivity increased significantly with an increase in temperature from 550 to 650 °C over Ni/TiO_2. Zhang et al.[14] reported that glycerol decomposition to CH_4 is highly favorable during the reforming process. Perhaps, Ni/TiO_2 is highly active in glycerol decomposition to CH_4 at higher temperatures compared to Ni/MgO and Ni/CeO_2. In contrast to Ni/TiO_2 and Ni/MgO, CH_4 selectivity decreased significantly with the increase in temperature over Ni/CeO_2. This is probably due to the fact that Ni/CeO_2 is also active in methane reforming compared to other catalysts. Methane selectivity was below 6% in all the catalysts. Likewise, CO_2 selectivity increased significantly with the increase in temperature over Ni/MgO and Ni/TiO_2 catalysts. However, CO_2 selectivity increased significantly with the increase in temperature from 550 to 600 °C and decreased significantly with further increase in temperature to 650 °C over Ni/CeO_2. As seen from the figure, the sum of CO, CH_4, and CO_2 selectivity is below 60% meaning that a substantial amount of carbon is either deposited in catalysts and/or in the reactor tube and/or converted into liquid products. Liquid products in the condensate were identified using a gas chromatograph-mass spectrometer (GC-MS). Some of the major products in the liquid were formaldehyde, acetaldehyde, ethanol, acetic acid, acetol, and propylene glycol.

The main objective of this study was to compare the effects of the supports. As seen in Figure 6b, it is difficult to

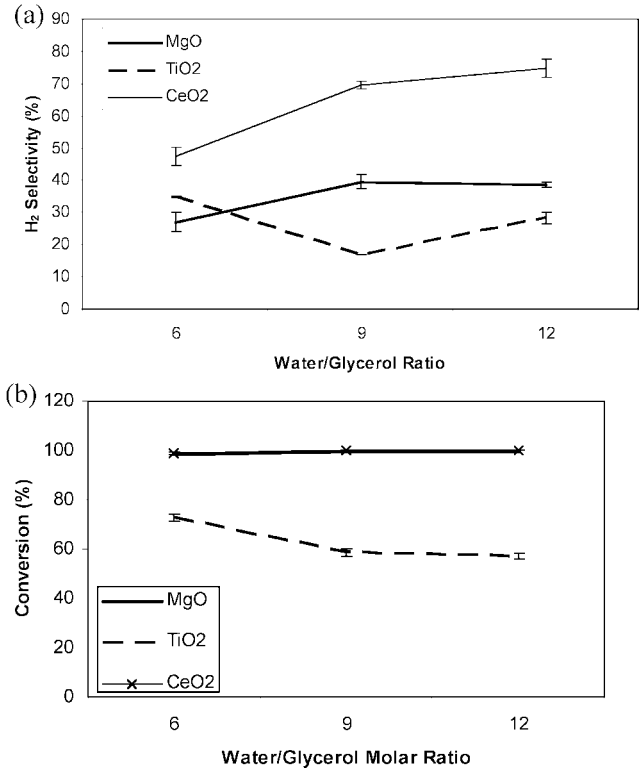

Figure 9. Effect of WGMR on (a) H_2 selectivity and (b) glycerol conversion at an FFR of 0.5 mL/min, catalyst loading of 0.75 g, and 600 °C (error bars equal 95% CI).

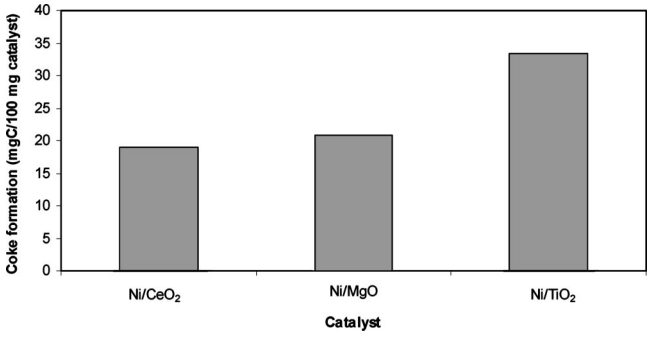

Figure 10. Coke formation on the selected catalysts after 2 h of operation at 550 °C, FFR of 0.5 mL/min, catalyst loading of 0.75 g, and WGMR of 12:1.

distinguish the effect of catalysts on glycerol conversion, especially for Ni/MgO and Ni/CeO_2. Therefore, we reduced the amount of the catalyst loading by 50% (i.e., 0.75 g) for clarity in comparison. Effects of FFRs on H_2 selectivity and glycerol conversion are discussed in Figure 8. The increase in FFR from 0.5 to 0.7 mL/min reduced H_2 selectivity significantly over Ni/TiO_2 and Ni/CeO_2 catalysts; whereas, H_2 selectivity did not reduce significantly with an increase in FFR from 0.5 to 0.6 mL/min over Ni/MgO. A further increase in FFR from 0.6 to 0.7 mL/min decreased H_2 selectivity significantly over Ni/MgO. Ni/CeO_2 showed the highest H_2 selectivity among Ni/MgO and Ni/TiO_2 catalysts. The hydrogen selectivity on Ni/CeO_2 was 47.3% and was reduced to 35.5% at an FFR of 0.5 and 0.7 mL/min, respectively. Glycerol conversion reduced significantly with an increase in FFR from 0.5 to 0.6 and 0.6 to 0.7 mL/min over the three catalysts tested in this study and was mainly due to the decrease in residence time. As we increased the FFR, the contact time with the catalysts reduced and lowered the glycerol conversion. There was no significant change in glycerol conversion between Ni/MgO and Ni/CeO_2 at an FFR of 0.5 and 0.6 mL/min. At 0.7 mL/min, Ni/CeO_2 showed the highest conversion followed by Ni/MgO and Ni/TiO_2. Glycerol conversion was 82.0% over Ni/CeO_2 at an FFR of 0.7 mL/min followed by 77.6% (Ni/MgO) and 47.0% (Ni/TiO_2). Ni/TiO_2 showed the lowest glycerol conversion in all FFRs tested.

Effects of WGMRs on H_2 selectivity and glycerol conversion are depicted in Figure 9. Hydrogen selectivity increased significantly by increasing WGMR from 6:1 to 9:1 and 9:1 to 12:1 over Ni/CeO_2. With the increase in WGMR from 6:1 to 9:1, H_2 selectivity increased significantly on Ni/MgO. With a further increase in WGMR from 9:1 to 12:1, H_2 selectivity did not increase significantly. On the other hand, H_2 selectivity decreased significantly by increasing WGMR from 6:1 to 9:1 and increased significantly with a further increase in WGMR from 9:1 to 12:1 on Ni/TiO_2. More analysis is needed before arriving at a proper conclusion regarding the "typical" behavior of Ni/TiO_2 found on this study. Ni/CeO_2 gave the highest H_2 selectivity (74.7%) followed by Ni/MgO (38.6%) and Ni/TiO_2 (28.3%) at WGMR of 12:1. Ni/CeO_2 showed the highest H_2 selectivity compared to Ni/MgO and Ni/TiO_2 at all WGMRs. The highest H_2 selectivity over Ni/CeO_2 was 74.7%, which corresponds to 5.22 mol of H_2 out of 7 mol (eq 1). Glycerol conversion remained the same with the increase in WGMR from 6:1 to 9:1 and 9:1 to 12:1 over Ni/MgO and Ni/CeO_2. Surprisingly, glycerol conversion reduced significantly with an increase in WGMR from 6:1 to 9:1 over Ni/TiO_2, but there was no significant change with an increase in WGMR from 9:1 to 12:1. In-depth analysis is required to find out whether there is any effect of excess water on the Ni/TiO_2 catalyst. Ni/MgO and Ni/CeO_2 showed similar activity in terms of glycerol conversion at different WGMRs. Ni/TiO_2, however, showed the lowest activity compared to CeO_2 and MgO supported Ni catalysts.

We found that the catalysts were more stable at higher temperature (650 °C) than at lower temperature (550 °C). Also, the gas flow rate was lower at 550 °C compared to that at 650 °C, which means that a significant amount of carbon was converted either to coke or in liquid products. Our results from total organic carbon and GC-MS analysis (not shown here) showed that glycerol was also converted to other organic compounds during the reforming process. We, however, did not quantify the amount of each product present in the liquid phase. We measured coke formation in the catalysts during the glycerol reforming at 550 °C because the catalysts were deactivated in a short time at low temperature. The coke formation was the highest on Ni/TiO_2 (33 mg carbon/100 mg catalyst) followed by Ni/MgO (21 mg carbon/100 mg catalyst) and Ni/CeO_2 (19 mg carbon/100 mg catalyst) as seen in Figure 10. The lower activity of Ni/TiO_2 could be attributed to the higher coke formation during the reforming process. Higher coke formation on Ni/TiO_2 could be attributed to TiO_2 being more acidic compared to MgO and CeO_2.

Figures 6, 8, and 9 illustrate that the H_2 selectivity was the highest over Ni/CeO_2 in all the conditions investigated in this study. Glycerol conversion on Ni/CeO_2 was always higher compared to Ni/TiO_2 and higher than that of or similar to Ni/MgO. On the basis of the results, we concluded that Ni/CeO_2 was more active compared to Ni/MgO and Ni/TiO_2 for H_2 production from the glycerol steam reforming process.

Conclusions

The glycerol steam reforming process was performed over Ni/CeO_2, Ni/MgO, and Ni/TiO_2 catalysts. Catalysts were characterized by various techniques. Ni/CeO_2 had the highest

surface area and metal dispersion. Increase in reaction temperatures and WGMRs resulted in positive effects both on H_2 selectivity and glycerol conversion over Ni/MgO and Ni/CeO_2. Glycerol conversion increased with an increase in reaction temperature, while it decreased with an increase in WGMR over Ni/TiO_2. Increase in FFR reduced H_2 selectivity and glycerol conversion in all the catalysts. Ni/CeO_2 was found to be the best catalyst compared to Ni/MgO and Ni/TiO_2 at the reaction conditions investigated. The maximum H_2 selectivity was 74.7% with Ni/CeO_2 at a WGMR of 12:1, temperature of 600 °C, and FFR of 0.5 mL/min. Glycerol conversion was more than 99% at the same conditions over Ni/CeO_2.

EF700520F